A Novel Mesogen-Jacketed Liquid Crystalline Electroluminescent Polymer with Both Thiophene and Oxadiazole in Conjugated Side Chain

QIAN YANG, YIDING XU, HAO JIN, ZHIHAO SHEN, XIAOFANG CHEN, DECHUN ZOU, XINGHE FAN, QIFENG ZHOU

Beijing National Laboratory for Molecular Sciences, Key Laboratory of Polymer Chemistry and Physics of Ministry of Education, College of Chemistry and Molecular Engineering, Peking University, Beijing 100871, China

Received 3 December 2009; accepted 18 December 2009
DOI: 10.1002/pola.23908

ABSTRACT: Mesogen-jacketed liquid crystalline polymers (MJLCPs) with both electron-transport oxadiazole and hole-transport thiophene in the side chain were reported for their promising electroluminescent property. Monomers of 2,5-bis{5-[(4-alkoxyphenyl)-1,3,4-oxadiazole]thiophen-2-yl}styrene (M-C*m*, *m* is the number of the carbons in the alkoxy groups, $m = 8,10$) were synthesized and confirmed by ^{1}H-NMR, mass spectrometry, and elemental analysis. The corresponding polymers were successfully obtained and characterized by thermal analysis, optical spectroscopy, cyclic voltammetry, electroluminescent analysis, polarized light microscopy (PLM), and wide-angle X-ray diffraction (WAXD). The polymers exhibited high decomposition temperatures reaching 382 °C and high T_g's reaching 184 °C. The absorption spectra indicated that both the monomers and polymers had little aggregation in film than that in solution, and the absorption spectra of the polymers showed an obvious blue-shift compared with those of the monomers. Both the monomers and the polymers had blue-green emission, and the photoluminescence spectra of the polymers in film suggested the formation of excimer or exciplex. The polymers showed lower HOMO energy levels and LUMO energy levels than those of the MJLCPs containing oxadiazole unit reported before. Electroluminescence study with the device configuration of ITO/PEDOT/PVK/polymer/TPBI/Ca/Ag showed maximum brightness and current efficiency of 541 cd/m^2 and 0.10 cd/A, which proved that the introduction of directly connected electron- and hole-transport units could greatly improve the EL property of side-chain conjugated polymers. The phase structures of the polymers were confirmed to be smectic A phase through the results of PLM and WAXD. The annealed samples emitted polarized photoluminescence at room temperature, which indicated potential utility for practical applications in display. © 2010 Wiley Periodicals, Inc. J Polym Sci Part A: Polym Chem 48: 1502–1515, 2010

KEYWORDS: electroluminescence; mesogen-jacketed liquid crystalline polymers; oxadiazole; side-chain conjugated polymers; thiophene

INTRODUCTION Liquid crystalline electroluminescent (EL) polymers have aroused researchers' intense interest as the self-assembling nature of liquid crystals that gives improved carrier mobility and polarized emission when uniformly aligned,[1,2] and, therefore, the advantage of providing improved viewing in bright-light conditions, which is the irreplaceable advantage over conventional liquid crystal display. Nematic and smectic luminescent liquid crystals has the key advantages of high carrier mobility, polarized emission, and enhanced output-couping, and their self-assembling properties and supramolecular structures can be regulated to improve the performance of semiconductors.[3–6] In EL area, side-chain conjugated polymers are promising as they have not only the advantages of polymers, such as good film forming and easy processing property, but also the advantages of low molecular weight compounds, such as good solubility in common organic solvents, high purity, a variety of possible pendant groups, well-defined polymer architecture and a well-defined conjugation length as a result of carrying isolated luminescent functional groups in their side chains therefore the conjugation lengths can be controlled.

The side chain of MJLCP (mesogen-jacketed liquid crystalline polymer) is attached laterally to the main chain without or with only short spacer,[7–9] so the large hindrance of the bulky side chain can avoid the intermolecular aggregation, which is favorable for the high efficiency of the EL devices. The previous work in our group had attempted to introduce the electron-transport oxadiazole unit into the side chain of the MJLCPs, and such MJLCPs had better electron-transport property and the maximum brightness and external quantum efficiency could reach 290.8 cd/m^2 and 0.24%, respectively, when multilayer devices were used.[10]

Although in the processing of multilayer devices of light-emitting polymers, spin-coating is the most widely used method, and the existence of solvent makes the two functional layers permeated into each other, which makes the functional layer less effective. So we consider to introduce hole-transport thiophene group into the side chain further to

Correspondence to: X. H. Fan (E-mail: fanxh@pku.edu.cn) or Z. H. Shen (E-mail: zshen@pku.edu.cn) or Q.-F. Zhou (E-mail: qfzhou@pku.edu.cn)
Journal of Polymer Science: Part A: Polymer Chemistry, Vol. 48, 1502–1515 (2010) © 2010 Wiley Periodicals, Inc.

obtain better EL properties by balancing electrons and holes in molecular structure scale. Main-chain conjugated polymers with electron- and hole-transport segments directly connected in the main chain have been widely studied in the area of PLEDs (polymeric light-emitting diodes). For instance, Yu et al. synthesized light-emitting copolymers with *p*-dopable bithiophene and *n*-dopable oxadiazole group directly connected and alternated in the conjugated backbone, and the *n*-doping potential of the polymer was similar with that of oxadiazole-containing polymers, whereas its *p*-doping potential was comparable with that of the typical *p*-dope type polymers like poly(*p*-phenylenevinylene) (PPV) and polythiophenes (PT), which firstly presented a possible approach to balance the rates of injection of electrons and holes in PLEDs by designing the molecular structure so as to control the intrinsic properties of light-emitting materials.[11] Huang et al. devoted effort to the synthesis of oxadiazole-containing light-emitting polymers with thiophene rings directly connected with oxadiazole rings in the conjugated backbone and the fabrication of single-layer device to investigate the diode character.[12] Mochizuki et al. designed four electroactive polymers with oxadiazole directly connected with different arylamine moieties in the conjugated side chains, and all of the polymers emitted strong blue fluorescence, with the maximum luminance of 30 cd/m^2 for the EL device consisting of the polymer containing oxadiazole and triphenylamine groups.[13] So in this work, the two kinds of functional groups of thiophene and oxadiazole were designed to be connected directly expecting to realize highly efficient EL.

In this investigation, we report the synthesis of a novel class of electroluminescent MJLCPs with thiophene and oxadiazole directly connected in side chain with the aim of balancing the injection and transportation of both the holes and electrons. Their thermal, optical, electrochemical, and electroluminescent properties are discussed. Furthermore, as previous research in our group discovered that when the side chain was bulky enough, the polymers could form lamellar SmA phase in liquid crystalline state.[14,15] The polymers in this work own the largest π-conjugated system among the MJLCPs, so the liquid crystalline properties are studied in detail, either, with polarized light microscopy (PLM), 1D wide-angle X-ray diffraction (WAXD), and 2D WAXD used.

EXPERIMENTAL

Materials and Measurements

THF was heated under reflux over sodium/benzophenone and freshly distilled before use. Triethylamine was heated over potassium hydroxide for 22 h and distilled. DMF was dried over anhydrous $MgSO_4$ for 24 h and distilled under reduced pressure. CuBr was synthesized from $CuSO_4$, NaBr, and Na_2SO_3, and purified by washing in acetic acid and methanol, and then dried under vacuum before use. All other chemicals were purchased from Aldrich, Acros, and Alfa Aesar, and used without further purification.

All new compounds were identified by ^{1}H-NMR, mass spectroscopy, and elemental analysis (EA). The ^{1}H-NMR spectra were recorded with a Bruker ARX400 spectrometer at room temperature with deuterated chloroform ($CDCl_3$) as the solvent, and the chemical shifts were reported in ppm with tetramethylsilane (TMS) as the internal standard. Mass spectra were recorded on a Finnigan-MAT ZAB-HS spectrometer when molecular weight was under 800 and on a Bruker Daltonics Autoflex III MALDI-TOF spectrometer when molecular weight was higher than 800. Elemental analysis was carried out on an Elementar Vario EL instrument. The molecular weight and molecular weight distribution of the polymers were determined by gel permeation chromatography (GPC) on a Waters 2410 instrument equipped with three Waters μ-Styragel columns (10^3, 10^4, and 10^5 Å) in series, with THF as the eluent at a flow rate of 1.0 mL/min at 35 °C. Monodisperse polystyrene standards were used for calibration.

The thermogravimetric analysis (TGA) of the polymers was performed under nitrogen atmosphere and in the air both at a heating rate of 10 °C/min with a TA SDT Q600 analyzer. Differential scanning calorimetry (DSC) examination was carried out on a TA DSC Q100 calorimeter with a programmed heating procedure in nitrogen. The sample size was about 5 mg and encapsulated in hermetically sealed aluminum pans, whose weights were kept constant. The temperature and heat flow scale at different cooling and heating rates were calibrated using standard materials such as indium and benzoic acid. The glass transition temperatures (T_g) were obtained from the second heating curves.

Polarized light microscopy (PLM) observation was performed on a Leitz Laborlux 12 microscope with a Leitz 350 hot stage. The samples were cast from THF solution and slowly dried at room temperature.

One-dimensional (1D) wide-angle X-ray diffraction (WAXD) experiments were performed on a Philips X'Pert Pro diffractometer with an X'celerator detector and a 3 kW ceramic tube as the X-ray source (Cu Kα). The reflection peak positions were calibrated with silicon powder ($2\theta > 15°$) and silver behenate ($2\theta < 10°$). The sample stage of Philips X'Pert Pro was set horizontally, with the samples protected by nitrogen purge gas during the measurements, and a temperature control unit (Paar Physica TCU 100) in conjunction with the diffractometer was utilized to study the phase structure evolution with the varied temperature. The heating and cooling rates in the WAXD experiments were 5 °C/min and the sample temperature was controlled within ±1 °C.

Two-dimensional (2D) WAXD pattern was obtained using Bruker D8Discover diffractometer with GADDS as a 2D detector. The 2D diffraction patterns were recorded in a transmission mode at room temperature with oriented samples prepared by mechanically shearing from the LC phase when applicable. Silicon powder and silver behenate were used as standards again. The sample was positioned on the sample stage so that the mechanically shearing direction was perpendicular to the point-focused X-ray beam. For both the 1D and 2D diffractions, the background scattering was recorded and subtracted from the sample patterns.

Absorption spectra were measured with a PerkinElmer Lambda 35 UV–vis spectrophotometer, and PL spectra were obtained using a Hitachi F-4500 fluorescence spectrophotometer. The cyclic voltammograms were recorded with a voltammetric analyzer (model CHI630C from Shanghai Chenhua Instrument Co.) in solution of tetrabutylammonium perchlorate (0.1*M*) in acetonitrile with a scanning rate of 100 mV/s at room temperature under nitrogen atmosphere. The measuring cell consisted of vitreous carbon electrode as the working electrode, Ag/AgCl electrode as the reference electrode, and platinum wire electrode as the auxiliary electrode. The polymer films were coated on the working electrode by casting and then dried in air. The energy levels were calculated with the ferrocene (FOC) value of −4.8 eV with respect to vacuum level as a calibration reference. After the measurement, two drops of FOC in acetonitrile (3 m*M*) were added and measured for calibration. Therefore, the HOMO levels of the polymers could be calculated by the equation $E_{\mathrm{HOMO}} = -e\ (E_{\mathrm{onset(ox)}} - E_{1/2,\ \mathrm{FOC}}) - 4.8$ eV, and the LUMO level could be estimated by the equation $E_{\mathrm{LUMO}} = -e\ (E_{\mathrm{onset(red)}} - E_{1/2,\ \mathrm{FOC}}) - 4.8$ eV, where the $E_{1/2,\ \mathrm{FOC}}$ standards for the half-wave potential of F_c/F_c^+.

Fabrication of the PLED Devices

Multilayer light-emitting diodes with the configuration of ITO/PEDOT/polymer/TPBI (15 nm)/Mg:Ag (10:1, wt %)/Ag and ITO/PEDOT/PVK/polymer/TPBI (15 nm)/Ca (25 nm)/Ag (80 nm) were fabricated for the investigation of optoelectronic characteristics. The patterned indium tin oxide (ITO) glass substrate was cleaned in turn with substrate-cleaning detergent, deionized water, acetone, and ethanol for 15 min under ultrasonic condition, and finally treated with UV-ozone for about 25 min. Then a hole-injection layer of PEDOT was spin-coated on it and dried by baking in air at 120 °C for 10 h. PVK was spin-coated from 1,1,2,2-tetrachloroethane solution (10 mg/mL) and dried by baking in air at 150 °C for 2 h. Then the emitting layer was spin-cast onto the PVK layer from toluene solution (10 mg/mL) through a 0.45 μm Teflon filter. The thickness of the spin-coated film was controlled by regulating the spinning speed. Finally, the coated ITO was transferred into a deposition chamber with a base pressure of 1×10^{-6} Torr, TPBI and metal layer was evaporated onto the polymer layer. The emitting area was 2 mm × 2 mm. The EL spectra were measured with a spectrofluorometer FP-6200 (JASCO). A source-measure unit R6145 (Advantest), multimeter 2000 (Keithley), and luminance meter LS-110 (Minolta) were used for *I-V-L* measurements. Relative luminance was directly detected by using a multifunctional optical meter 1835-C (Newport). All of the fabrication and characterization of the light-emitting diode devices was performed in air and at room temperature without protective encapsulation.

Synthesis of the Monomers

The synthetic routes of the monomers of 2,5-bis{5-[(4-alkoxyphenyl)-1,3,4-oxadiazole]thiophen-2-yl}styrene (M-C*m*, *m* is the number of the carbons in the alkoxy groups, *m* = 8,10) were depicted in Scheme 1. The experimental details were described later taking M-C10 as an example.

Ethyl 2-thiophenecarboxylate 1

To a stirred solution of 2-thiophenecarboxylic acid (15.38 g, 0.12 mol), ethanol (5.52 g, 0.12 mol) and 4-dimethylaminopyridine (DMAP) (0.36 g, 3.00 mmol) in dried dichloromethane (DCM) (270 mL), a solution of *N*,*N*′-dicyclohexylcarbodiimide (DCC) (24.76 g, 0.12 mol) in DCM (30 mL) was added. The reaction mixture was stirred at room temperature, with or without the protection of dry argon, for 24 h. The floating solid was then filtered and the solvent was removed by distillation under reduced pressure. The crude product was purified by column chromatography (silica gel) with dichloromethane as eluant to give a pale yellow oil. Yield: 76.3%. ^{1}H-NMR ($CDCl_3$, δ, ppm): 7.79–7.80 (d, 1H, Ar—H), 7.53–7.54 (d, 1H, Ar—H), 7.08–7.09 (d, 1H, Ar—H), 4.32–4.39 (t, 2H, —OCH_2—), 1.35–1.40 (t, 3H, —CH_3).

Ethyl 5-(tri-n-butylstannyl)-2-thiophenecarboxylate 2

To a stirred solution of diisopropylamine (1.01 g, 10.00 mmol) in dry THF (30 mL) at −78 °C under an atmosphere of dry argon, *n*-butyllithium (4 mL, 2.5*M* solution in hexane, 10.00 mmol) was added by syringe. The reaction mixture was stirred for 1 h, and then a solution of compound **1** (1.56 g, 10.00 mmol) in dry THF (3 mL) was added by syringe, with the temperature kept at −78 °C. After stirring for another 1 h, a solution of tri-*n*-butylstannyl chloride (3.26 g, 10.00 mmol) in dry THF (4 mL) was added by syringe, with the temperature still kept at −78 °C. After the addition, the reaction mixture was stirred at −78 °C for 1 h, and then allowed to reach room temperature and react overnight. It was then carefully quenched with water (40 mL) and the organic layer was separated. The aqueous phase was washed with dichloromethane (3 × 40 mL) and the combined organic extract was then dried over anhydrous $MgSO_4$. The crude product was purified by column chromatography (silica gel) with dichloromethane/petrol ether 1:3 (v/v) as eluant to give a colorless oil. Yield: 72.3%. ^{1}H-NMR ($CDCl_3$, δ, ppm): 7.88–7.89 (d, 1H, Ar—H), 7.14–7.15 (d, 1H, Ar—H), 4.31–4.38 (t, 2H, —OCH_2—), 0.87–1.61 (m, 30H, —CH_3, —$CH_2CH_2CH_2CH_3$). MS (*m*/*z*): 446.

2,5-Bis[(5-ethoxycarbonyl)thiophen-2-yl]styrene 4

To a mixture of bis (triphenylphosphine) palladium (II) chloride (0.84 g, 1.20 mmol) and hydroquinone (0.08 g) in DMF (70 mL) at 100 °C under argon atmosphere, compound **2** (13.38 g, 30.00 mmol) and compound **3** (3.87 g, 15.00 mmol) in dry DMF (50 mL) were added by syringe in order, and the reaction mixture was stirred for 24 h. Then the mixture was washed with hydrochloric acid (6 vol %, 300 mL) and dichloromethane to remove the high boiling DMF and extract the product from the aqueous phase. Then the organic phase was washed by $NaHCO_3$ saturated aqueous solution (200 mL) to be neutralized. After removing the solvent under reduced pressure and drying over anhydrous $MgSO_4$, the residue was subjected to column chromatography (silica gel) with dichloromethane/petrol ether 2:1 (v/v) as eluant to get a pale yellow solid. Yield: 68.0%. ^{1}H-NMR (400 MHz,

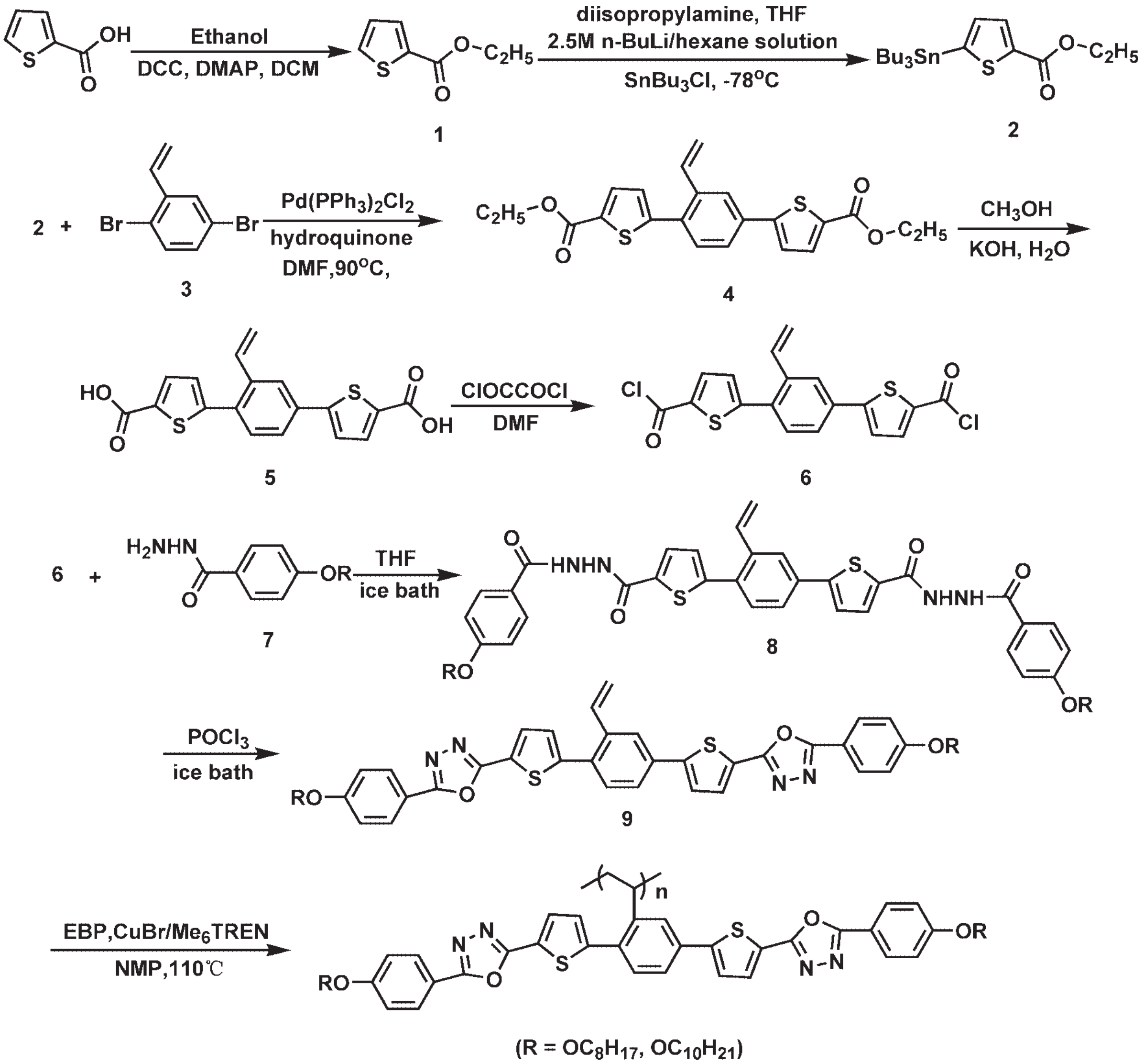

SCHEME 1 Synthetic route of monomers and polymers.

$CDCl_3$, δ, ppm): 7.84–7.85 (d, 1H, phenyl-H), 7.78–7.80 (t, 2H, thiophene-H), 7.58–7.61 (t, 1H, phenyl-H), 7.47–7.50 (d, 1H, phenyl-H), 7.37–7.38 (d, 1H, thiophene-H), 7.10–7.11 (d, 1H, thiophene-H), 6.92–7.01 (t, 1H, —CH═), 5.78–5.84 (d, 1H, $=CH_2$), 5.38–5.43 (d, 1H, $=CH_2$), 4.33–4.42 (t, 4H, $—OCH_2—$), 1.37–1.43 (t, 6H, $—CH_3$). MS (*m*/*z*): 412.

2,5-Bis(5-carboxythiophen-2-yl)styrene 5

The compound **4** (2.10 g, 5.00 mmol), hydroquinone (0.50 g), and methanol (200 mL) were put into a 500 mL flask, as the compound **4** was reluctant to dissolve completely in methanol, the mixture was heated to reflux. After the mixture appeared homogeneous, KOH aqueous solution (20 wt %, 90 mL) was added. After 3 h, dilute hydrochloric acid was added into the solution until the PH reached 2. The generated solid was then collected and washed with water and methanol. The final product appeared to be dark yellow powder. Yield: 97.6%. ^{1}H-NMR (DMSO-d_6, δ, ppm): 13.23 (s, 2H, —COOH), 7.97–7.98 (d, 1H, phenyl-H), 7.70–7.77 (m, 3H, thiophene-H), 7.57–7.60 (d, 1H, phenyl-H), 7.52–7.54 (d, 1H, phenyl-H), 7.24–7.25 (d, 1H, thiophene-H), 6.90–6.99 (t, 1H, —CH═), 5.99–6.04 (d, 1H, $=CH_2$), 5.45–5.49 (d, 1H, $=CH_2$). MS (*m*/*z*): 356.

2,5-Bis(5-chlorocarbonylthiophen-2-yl)styrene 6

With **5** (1.06 g, 3.00 mmol) and oxalyl chloride (80 mL) well mixed, several drops of dried DMF were added as catalyst. The reaction mixture was stirred at room temperature for quite a long time until the mixture turned to be homogeneous. The excess of oxalyl chloride was removed under reduced pressure and then carried away completely with the addition of petrol ether to afford a yellow solid. The product was sealed and kept dry.

p-Alkoxybenzhydrazide 7

This compound was synthesized according to the procedure we reported before.[14]

2,5-Bis[5-(4-decyloxyphenyl-bishydrazide)thiophen-2-yl]styrene 8

To the intensely stirred solution of **7** (3.31 g, 11.34 mmol) in dry THF (50 mL), hydroquinone (0.10 g), and triethylamine (10 mL) were added. The solution of **6** (2.23 g, 5.67 mmol) in dry THF (80 mL) was slowly dropped at the temperature of ice bath. A great deal of suspended white solid generated immediately and its color turned darker when the reaction proceeded further, and the reaction mixture was stirred at room temperature for another 24 h after the addition. Then the solvent was removed under reduced pressure, and the residue was dispersed with water and neutralized to gain dark yellow solid. As the product could hardly dissolved in any common organic solvent, no further purification was performed.

2,5-Bis{5-[(4-decyloxyphenyl)-1,3,4-oxadiazole]thiophen-2-yl}styrene 9 (M-C10)

The aforementioned **8** (14.37 g), hydroquinone (1.47 g), and phosphorus oxychloride (350 mL) were mixed and heated to reflux for 18 h. The cooled mixture was poured slowly into excessive ice water with intense stirring, and a great deal of solid generated rapidly. Then sodium hydroxide aqueous solution was added to neutralize the mixture, and the solid was filtered, washed with water and dried under vacuum. The crude product was purified firstly by column chromatography (silica gel) with dichloromethane/ethyl acetate 10:1 (v/v), and then by recrystallization in THF to yield a bright yellow powder (2.34 g, 17.0%). ^{1}H-NMR (400 MHz, $CDCl_3$, δ, ppm): 8.02–8.05 (d, 4H, phenyl-H), 7.84 (s, 1H, phenyl-H), 7.76–7.77 (d, 2H, thiophene-H), 7.59–7.60 (d, 1H, phenyl-H), 7.52–7.53 (d, 1H, phenyl-H), 7.43–7.44 (d, 1H, thiophene-H), 7.18–7.19 (d, 1H, thiophene-H), 6.99–7.02 (p, 5H, phenyl-H, $-CH=$), 5.82–5.87 (d, 1H, $=CH_2$), 5.44–5.47 (d, 1H, $=CH_2$), 4.00–4.04 (t, 4H, $-OCH_2-$), 1.78–1.85 (p, 4H, $-OCH_2CH_2-$), 1.44–1.51 (p, 4H, $-CH_2CH_3$), 1.28–1.33 (d, 24H, $-CH_2CH_2CH_2-$), 0.87–0.90 (t, 6H, $-CH_3$). Anal. Calcd. for $C_{52}H_{60}N_4O_4S_2$: C, 71.86; H, 6.96; N, 6.45. Found: C, 71.69; H, 7.01; N, 6.41. MS (MALDI) m/z: 869.6 (calcd. for $C_{52}H_{60}N_4O_4S_2$, 869.2).

Basic characterizations of **M-C8** are as follows: ^{1}H-NMR (400 MHz, $CDCl_3$, δ, ppm): 8.05–8.07 (d, 4H, phenyl-H), 7.88 (s, 1H, phenyl-H), 7.80–7.81 (d, 2H, thiophene-H), 7.63–7.66 (d, 1H, phenyl-H), 7.54–7.57 (d, 1H, phenyl-H), 7.46–7.47 (d, 1H, thiophene-H), 7.20–7.22 (d, 1H, thiophene-H), 6.99–7.08 (p, 5H, phenyl-H, $-CH=$), 5.83–5.89 (d, 1H, $=CH_2$), 5.44–5.48 (d, 1H, $=CH_2$), 4.02–4.06 (t, 4H, $-OCH_2-$), 1.78–1.87 (p, 4H, $-OCH_2CH_2-$), 1.48–1.49 (d, 4H, $-CH_2CH_3$), 1.25–1.33 (d, 16H, $-CH_2CH_2CH_2-$), 0.88–0.90 (t, 6H, $-CH_3$). Anal. Calcd. for $C_{48}H_{52}N_4O_4S_2$: C, 70.90; H, 6.45; N, 6.89. Found: C, 70.34; H, 6.75; N, 6.55. MS (MALDI) m/z: 813.3 (calcd. for $C_{48}H_{52}N_4O_4S_2$, 813.1).

Polymerization

Atom transfer radical polymerization (ATRP) was used to obtain the polymers. Typically, CuBr (1.44 mg, 0.01 mmol), a solution of ethyl 2-bromo-2-methylpropionate (EBP) (1.95 mg, 0.01 mmol) and 1,1,4,7,10,10-hexamethyltriethylenetetramine (Me_6TREN) (2.30 mg, 0.01 mmol) in *N*-methyl pyrrolidone (NMP) (0.80 g), M-C10 (0.87 g, 1.00 mmol), and NMP (4.45 g) were placed in a well-dried glass tube with a magnetic stir bar in sequence. Then the reaction mixture was purged with dry nitrogen and subjected to three freeze-pump-thaw cycles and sealed under vacuum. The tube was placed into an oil bath thermostatic at 110 °C. After 4 days, the tube was broken after the polymerization was terminated by putting the tube into ice/water mixture. The reaction mixture was diluted with THF, passed through a basic alumina column to remove the copper complex and precipitated in methanol. As the solubility of M-C10 in methanol was not good, the precipitate was redissolved in THF and reprecipitated twice by controlling the addition of methanol to eliminate the unreacted monomers. Finally, the polymer was dried under vacuum to a constant weight.

RESULTS AND DISCUSSION

Synthesis and Characterization of Monomers and Polymers

As shown in Scheme 1, the monomers were mainly synthesized in seven steps. In the synthesis of compound **1**, we also had a try that the reaction was performed in argon atmosphere, and it was found that the yield was 10% higher than that in the common condition. The synthesis of compound **4** was the crucial step in the entire synthesis of the monomers, which directly influenced the purity of the next products. Stille cross-coupling was used, which contained two important steps: synthesis of organotin reagents and process of cross-coupling.[16] The synthesis of organotin reagents needed to be performed in absolutely anhydrous and inert atmosphere at −78 °C, and diisopropylamine was added to stabilize the lithium complex. The color change was fairly obvious and was used to judge whether the reaction was successful or not: After the solution of compound **1** was added to the system, the color of the mixture changed to yellow-green and became darker as the addition continued, and finally became black completely. When tri-*n*-butylstannyl chloride was added, the color of the mixture turned yellow, and when the temperature rise to room temperature, the color of the mixture turned darker again, and became dark red in the end. In the cross-coupling step, it was unavoidable that homo-coupled product generated, which was in agreement with the statement in the literature.[17] In our synthesis, the homo-coupled product was removed by careful separation through column chromatography. Because vinyl group was unstable in high temperature as thermal polymerization might occur, hydroquinone was always added in the reaction mixture as polymerization inhibitor. In the synthesis of compound **6**, oxalyl chloride was used in stead of thionyl chloride, as the reaction could be performed under room temperature in stead of under reflux. Compound **8** had very high polarity and rather poor solubility in common solvents, so no further purification was carried out. The solubility of compound **9** was rather poor, too, which may be due to the large rigidity of the molecule, so dry method was used in column packing in stead of wet method to get better

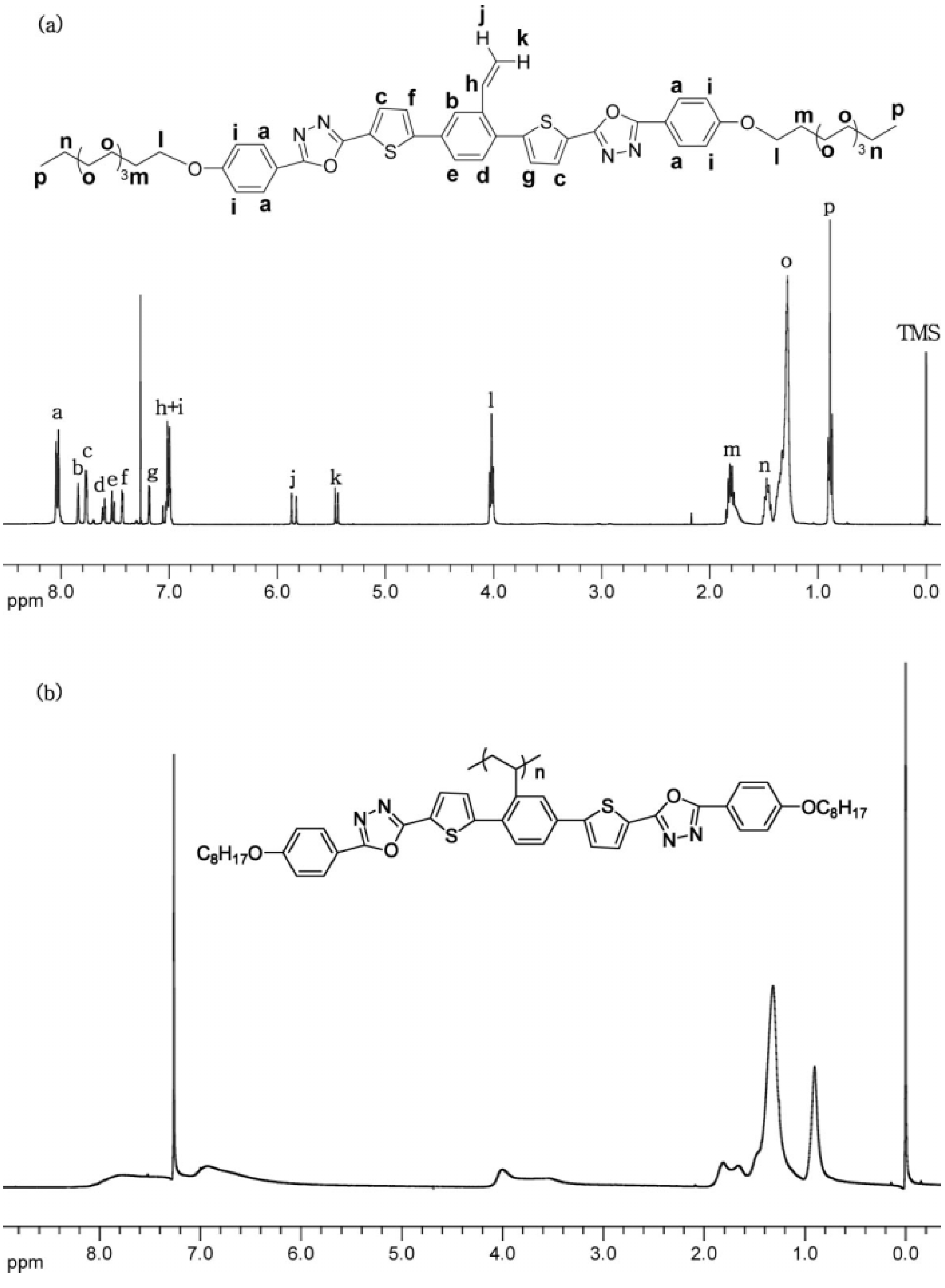

FIGURE 1 ^{1}H-NMR spectra of (a) the monomer M-C10 and (b) the polymer P-C8 in $CDCl_3$.

separation efficiency, and pure monomers were obtained after recrystallization in THF. The uncertainty in the last step of cyclization and the poor solubility induced the yield of pure monomers largely decreased. However, the successful synthesis and accumulation of sufficient amount of the monomers to polymerize was exciting. The structures of the monomers had been confirmed by ^{1}H-NMR, mass spectrometry, and elemental analysis.

ATRP method was used to get the corresponding polymers. As the oxadiazole rings could coordinate with the catalyst of

TABLE 1 Polymerization Results and Thermal Properties of the Polymers

Polymer	M_n ($\times10^4$)[a]	M_w ($\times10^4$)[a]	PDI[a]	T_d (°C)[b]	T_d (°C)[c]	T_g (°C)[d]
P-C8	0.8	0.9	1.22	378	359	184
P-C10	1.2	1.8	1.55	382	350	174

[a] M_n, M_w, and PDI of the polymers were determined by GPC using polystyrene standards in THF solutions.

[b] Temperature at 5 wt % loss under nitrogen atmosphere determined by TGA at a heating rate of 10 °C/min.

[c] Temperature at 5 wt % loss in air determined by TGA at a heating rate of 10 °C/min.

[d] Glass-transition temperature determined by DSC in nitrogen in the second heating curve at a heating rate of 20 °C/min.

CuBr, Me_6TREN was used as a stronger ligand. NMP was used as solvent in polymerization instead of the mostly used chlorobenzene, as the monomers with such a long conjugation had better solubility in elevated temperatures than that in other familiar solvents. The polymers were then successfully obtained, as the spectra of ^{1}H-NMR shown, the signals of the vinyl group at 5.4, 5.8, and 7.0 ppm in part (a) of Figure 1 completely disappeared in part (b), indicating the successful polymerization, and the broad peaks in part (b) of Figure 1 were consistent with the expected polymer structure. The low polymerization reactivity of the monomers induced longer reaction time (several days) and slightly higher polydispersity than what was observed for simple monomers such as styrene, due to the large delocalization of the radicals.[18] The polymers were completely soluble in the common organic solvents such as chloroform, THF, chlorobenzene, and dichloromethane, and they showed much better solubility than the corresponding monomers. The characterization results of the polymers were listed in Table 1.

Thermal Properties

Thermal properties of the polymers were evaluated by TGA and DSC, and the results were summarized in Table 1. The thermal stability of the polymers was investigated with TGA in both nitrogen and air (Fig. 2). The temperatures at 5 wt % loss were 378 °C and 382 °C for P-C8 and P-C10 in nitrogen, respectively. This series of polymers had fairly high decomposition temperatures even in air, with the temperatures at 5 wt % loss at 359 °C and 350 °C for P-C8 and P-C10, respectively, indicating that the polymers were quite stable at elevated temperatures, which was valuable in the application as optoelectronic devices and in heat treating in the study of liquid crystalline phase structures. DSC was performed to measure glass transition temperatures (T_g) of the polymers. The polymers had T_g's at about 184 °C and 174 °C, respectively, which were much higher than that of the polystyrene backbone and the MJLCPs reported before,[14,15] which indicated that the introduction of the pendant large waist-attaching side chain made the polymers more rigid. In general, high decomposition temperatures and high T_g's were advantageous for the polymers to be used as emissive materials in PLEDs.[19]

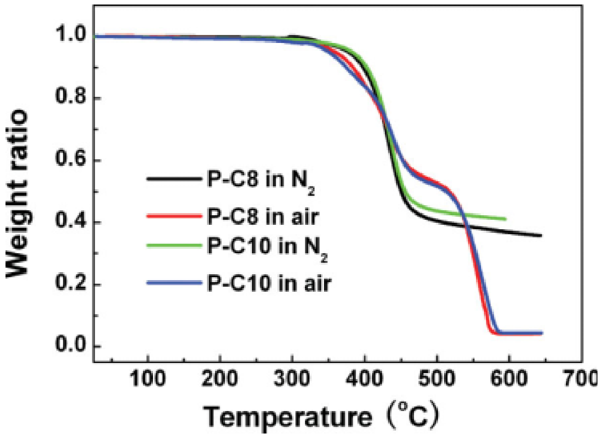

FIGURE 2 TGA plots of the polymers with a heating rate of 10 °C/min under nitrogen atmosphere and in air. [Color figure can be viewed in the online issue, which is available at www.interscience.wiley.com.]

Liquid Crystalline Properties

To investigate the phase structure of the polymers, PLM, 1D WAXD, and 2D WAXD experiments of P-C10 were performed.

Birefringence of the polymers were observed with PLM. The samples were cast from THF solution and slowly dried at room temperature. The birefringence appeared when the sample P-C10 was heated to 180 °C, which was a little higher than T_g (Fig. 3). When cooled to room temperature, the birefringence remained. So it was implied that the ordered structure formed at high temperature kept unchanged upon cooling, which was similar to some MJLCPs synthesized in our group before.[15,20,21]

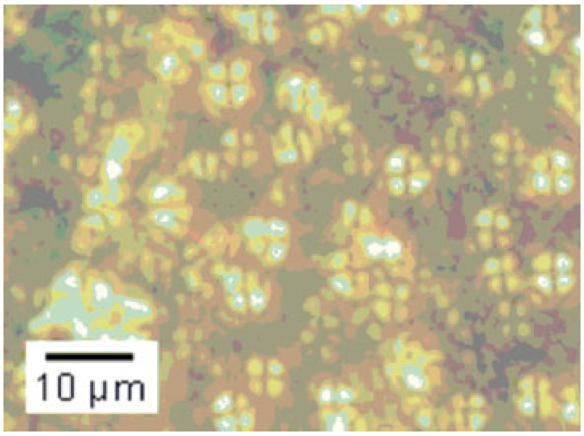

FIGURE 3 PLM image of P-C10 taken at 240 °C. [Color figure can be viewed in the online issue, which is available at www.interscience.wiley.com.]

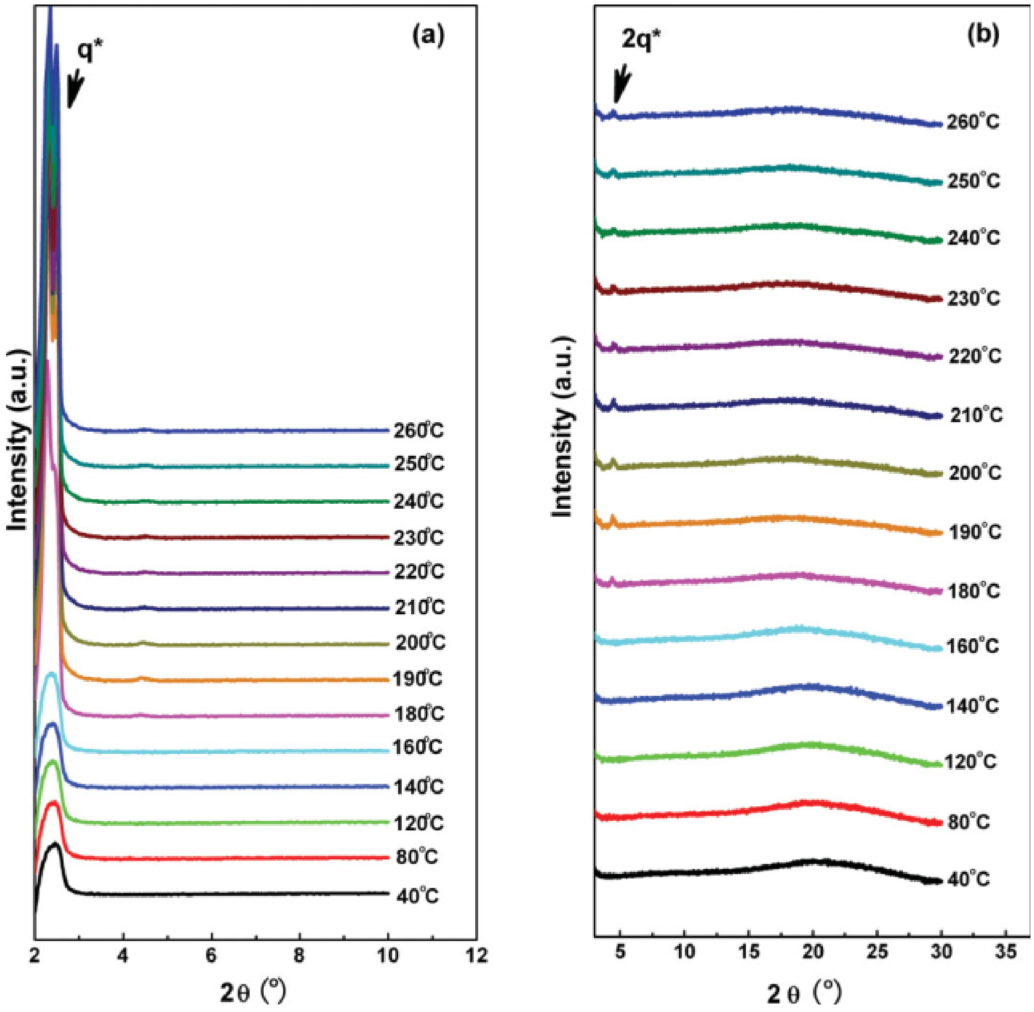

FIGURE 4 1D WAXD patterns of sample P-C10 obtained during the first heating (a) and partial pattern of 2θ from 4° to 30° (b) of the as-cast film. [Color figure can be viewed in the online issue, which is available at www.interscience.wiley.com.]

1D WAXD was used to investigate the phase transition and phase structure further. About 50 mg of polymer was dissolved in THF and cast onto a copper substrate, and then the solvent was allowed to evaporate slowly at room temperature. Figure 4 showed the 1D WAXD patterns of P-C10 from 40 to 260 °C at programmed temperatures. When the temperature reached 180 °C, a diffraction peak appeared, and the intensity of the peak increased when the heating was continued. At the same time, a higher-order diffraction peak was observed, too. At 230 °C, the position of the two diffraction peaks had 2θ values of 2.26° and 4.38°. The ratio of scattering vectors of these two peaks was ∼1:2, indicating a smectic structure of the sample. When the sample was cooled, the smectic phase was unchanged. The maximum *d*-spacing value was 3.90 nm, and it was a little less than 4.7 nm of the calculated length of the monomers with their alkoxy tails in stretched conformation. That was because the length of the flexible alkoxy chain was calculated as rigid conformation, and the flexible alkoxy groups also had the trend of interpenetrating with each other after the polymer entered liquid crystalline phase.[21] There were always

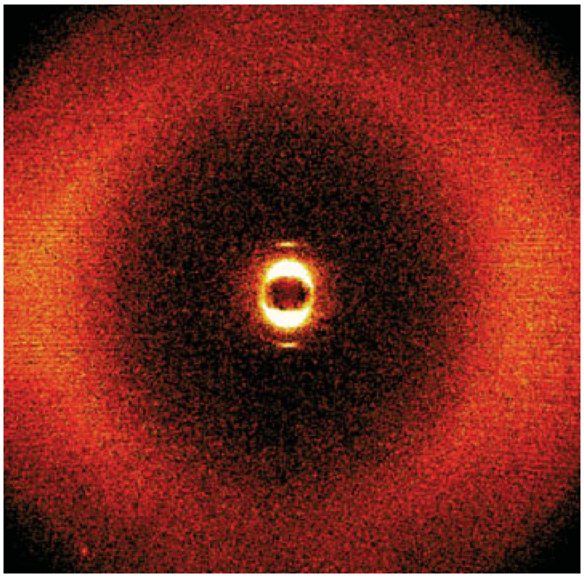

FIGURE 5 2D WAXD pattern of annealed P-C10 film recorded at room temperature. [Color figure can be viewed in the online issue, which is available at www.interscience.wiley.com.]

TABLE 2 Optical Properties of Monomers and Polymers in Chloroform Solutions and Solid Films

	Solution[a]			Film[b]	
Sample	Absorption λ_{max} (nm)	PL λ_{max} (nm)[c]	ϕ_{PL}[d]	Absorption λ_{max} (nm)	PL λ_{max} (nm)[c]
M-C8	371	437, 464	0.48	388	495, 511
P-C8	358	446, 462	0.38	360	519
M-C10	372	437, 461	0.52	375	521
P-C10	358	450, 464	0.29	359	498

[a] In chloroform ($1 \times 10^{-5}M$ for monomers and 1 mg/10 mL for polymers).

[b] Films were spin-cast from toluene solutions.

[c] Excitation wavelength was the maximum absorption wavelength.

[d] Fluorescence quantum efficiencies were measured in chloroform relative to quinine sulfate ($\phi_{PL} = 0.55$).

scattering halos at the 2θ of around 20° corresponding to the distance of 0.44 nm, which arise from the π–π stacking of the aromatic rings in the side chain, and was attributed to the lateral distance between the side chains within the layer. The positions of the halos slightly shifted toward lower angles upon the heating as a result of thermal expansion.

As for the phase structure would be smectic A or smectic C, 2D WAXD measurements were performed for annealed samples to confirm the phase structure. As the pattern in Figure 5 showed, when X-ray incident beam was incident, a pair of sharp diffraction arcs appeared on the meridian direction at $2\theta = 2.20°$ (*d*-spacing is 4.02 nm), and the second-order diffraction could be observed clearly at $2\theta = 4.30°$ (*d*-spacing is 2.06 nm), which indicated that the ordered structure was developed on the nanometer scale. Meanwhile, two scattering halos in the high 2θ angle arising from the π–π stacking of the aromatic rings in the side chains were more or less concentrated on the equator direction with rather broad azimuthal distributions. This revealed that only the short-range orders exist.[22] Similar results were obtained from P-C8, and the position of two diffraction peaks had 2θ values of 2.39° and 4.67° corresponding to the maximum *d*-spacing value of 3.69 nm, with the calculated length of 4.39 nm.

Combining the 1D WAXD results and the 2D WAXD pattern style, it was concluded that such polymers as P-C10 and P-C8 formed SmA phase after the liquid crystalline phase transition (Fig. 6).

Photophysical Properties

The photophysical characteristics of the polymers were investigated both in chloroform and as films cast from toluene solutions. The photophysical properties of the monomers were also discussed as the molecular structures of monomers reflected those of the repeat units of the polymers. Their absorption and emission spectral data are summarized in Table 2. Figures 7 and 8 display the absorption and photoluminescence (PL) spectra both in solution and film state. The UV–vis absorption spectra (Fig. 7) of the monomers and polymers in solution were recorded at room temperature in chloroform, which was a relatively nonpolar solvent to make sure the interaction between the solute molecules and the solvent was little. The absorption spectra in film were performed after the toluene solutions were spin-coated on a quartz plate. The absorption maximum of M-C8 and M-C10 in solution was at 371 and 372 nm, whereas at 388 and 375 nm in film, respectively. The absorption maximum of M-C8 in film red-shifted 17 nm than that in solution, which was much larger than the 3 nm red shift of M-C10, which indicated that M-C8 was easier to aggregate than M-C10, due to the less bulky tails. The absorption maximum of P-C8 and P-C10 in solution were both at 358 nm and were at 360 and 359 nm in film, respectively, which suggested that the molecular arrangement of polymer chains was almost the same both in solution and in thin film, indicating that the polymers lacked order even in the solid state, and the aggregation of the polymers in film was not very great, either, from which it was inferred that the polymer backbone limited the motions of the side chains. It was worth noticing that the absorption spectra of the polymers showed an obvious blue-shift compared with those of the corresponding monomers, which was ascribed to the loss of conjugation of the vinyl group with the directly connected aromatic rings.[23]

The photoluminescence spectra of monomers and polymers were recorded both in chloroform solution and in film, too. They were both blue-emitters. In solution, the emission bands were at 437 and 464 nm for M-C8 and 437 and 461 nm for M-C10, and at 446 and 462 nm for P-C8 and 450 and 464 nm for P-C10, respectively. Although in film state, the emission bands of the two monomers were at 495 and 511 nm and 521 nm, respectively, and those of the two polymers were at 519 and 498 nm, respectively. The emission of the polymers in film had a great red-shift of about 50 nm relative to that in solution, and the red shift of the emission of monomers in film were even larger than those of the polymers, to be 60–80 nm, which was ascribed to the strong intra- or inter-chain interaction and the generation of excimer or exiplex that provided nonradiation decay channels for the excited states.[24–28] The maximum emission of M-C10 was 26 nm red-shifted than that of M-C8, which was attributed to its greater tendency of recrystallization and subsequent energy dissipation in nonradiative transition, which caused the emission red-shift, due to its longer tails, therefore, better mobility.[29] The maximum emission of P-C8 was situated at 519 nm and was 21 nm red-shifted than that of P-C10, which was ascribed to the great intermolecular interaction besides the intramolecular interaction as a result of the shorter alkoxy tails.

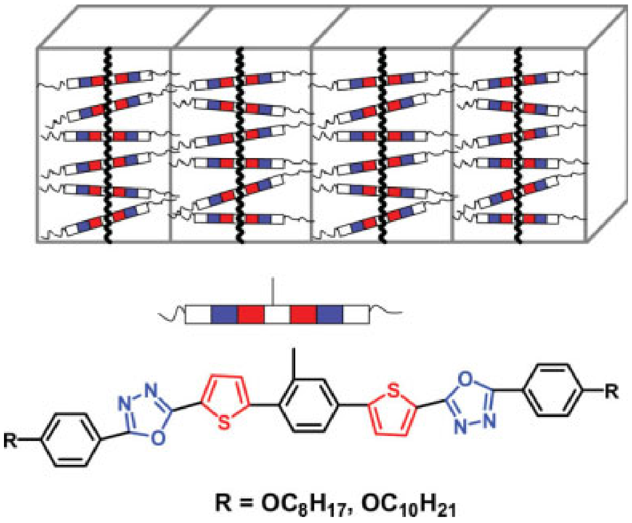

FIGURE 6 Schematic drawing of the SmA layer structure of the polymers.

The quantum efficiencies of the monomers and polymers were measured in chloroform with quinine sulfate in dilute sulfuric acid as reference. The quantum efficiencies were 0.48 and 0.52 for M-C8 and M-C10, and those of the corresponding polymers were 0.38 and 0.29. The polymers had lower fluorescence quantum efficiencies than corresponding monomers, due to the concentration effect of the close side chains attached to the backbones.

Polarized Photoluminescence

To make use of the liquid crystalline self-assembling properties of the polymers, we demonstrated the polarized photoluminescence spectra of P-C10 film in Figure 9. The film was annealed at 220 °C for 6 h, and the polarized light entered the film in two perpendicular directions, the fluorescence intensity changed about 10 times. The thermal treatment was the same as that in 2D WAXD measurements, so such large difference was ascribed to the anisotropy in different directions resulted from the ordered structure in the annealed samples. Such tendency of forming ordered structure was expected to be favorable to the transportation of charge carriers and the potential utility for practical applications in the area of display. Similar considerations of introducing self-organized structures such as liquid-crystalline polymers have also been reported, and the improvement of the EL properties was ascribed to the bipolar carrier-transporting abilities of the LC molecules.[30,31] Moreover, high ordered phase structure was expected to replace N phase to facilitate the charge carrier transport,[32] which was realized in this investigation.

Electrochemical Properties

The electrochemical cyclic voltammetry was performed for determining the highest occupied molecular orbital (HOMO) and the lowest unoccupied molecular orbital (LUMO) energy levels of the polymers, which correspond to ionization potential (IP) and electron affinity (EA), respectively. Figure 10 shows the cyclic voltammograms of the polymer films, and all related electrochemical data are summarized in Table 3. The onset oxidation potentials were situated at 1.66 V for P-C8 and 1.77 V for P-C10, from which their HOMO levels were estimated to be −6.07 and −6.18 eV, respectively, according to the equation $\mathrm{IP} = -e(E_{\mathrm{onset(ox)}} - E_{1/2,\ \mathrm{FOC}}) - 4.8$ eV. The onset reduction potentials were situated at −1.19 V for P-C8 and −1.36 V for P-C10, with their LUMO levels estimated to be −3.22 and −3.05 eV according to the equation $\mathrm{EA} = -\mathrm{e}(E_{\mathrm{onset(red)}} - E_{1/2,\ \mathrm{FOC}}) - 4.8$ eV. From the HOMO and LUMO levels, the band gaps of the P-C8 and P-C10 were estimated to be 2.85 and 3.13 eV, respectively.

The LUMO energy levels were much lower than those of the MJLCPs containing electron-transport oxadiazole in the side chains reported before,[10] which indicated that the electron injection and transportation was improved further. The HOMO energy levels decreased, too, which was consistent with the results that the LUMO and HOMO energy levels both lower when thiophene was introduced into the conjugated side chain,[33] as a result of the increased electron-

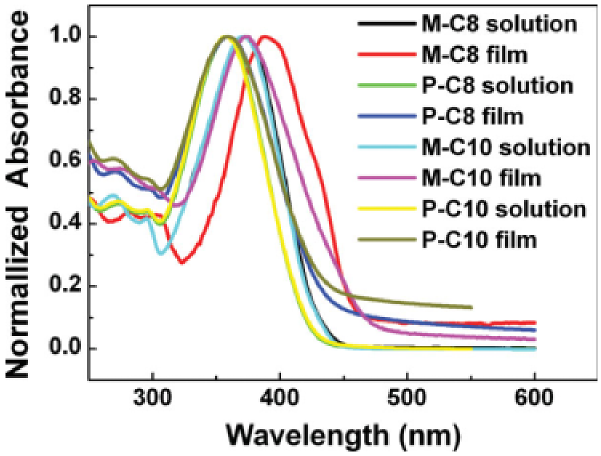

FIGURE 7 Normalized UV–vis absorption spectra of monomers (1 × 10^{-5}*M*) and polymers (1 mg/10 mL) in chloroform solutions and film state measured at room temperature.

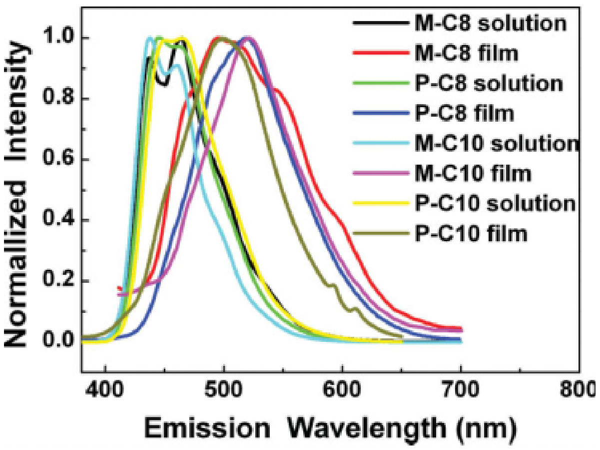

FIGURE 8 Normalized PL spectra of monomers (1 × 10^{-5}*M*) and polymers (1 mg/10 mL) in chloroform solutions and film state measured at room temperature.

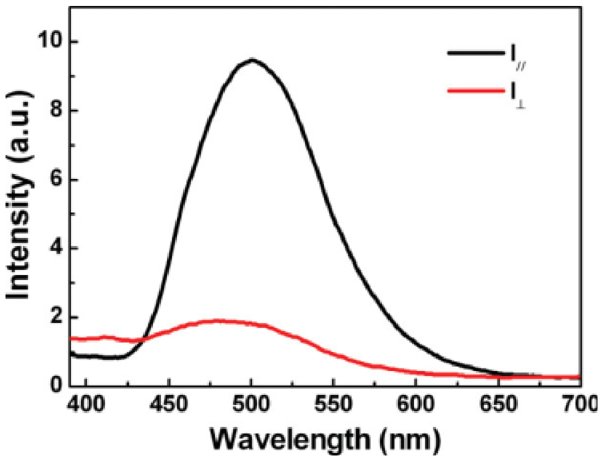

FIGURE 9 Polarized photoluminescence spectra of P-C10 film. $I_{//}$ and $I_{\perp}$ denoted the fluorescence polarized in two perpendicular directions. [Color figure can be viewed in the online issue, which is available at www.interscience.wiley.com.]

withdrawing characteristic of the pendant side chains. The electrochemical band gaps were consistent with the optical band gaps on the whole, and larger in a certain extent, because of the interface barrier for charge injection, which was in agreement with those observed in main-chain conjugated polythiophenes.[34]

Electroluminescent Properties

EL devices of P-C10 with different configurations were fabricated and taken as examples to investigate the optoelectronic characteristics of such kinds of MJLCPs, and the data were summarized in Table 4. At first, device a with the configuration of ITO/PEDOT/polymer/TPBI (15 nm)/Mg:Ag (10:1, wt %)/Ag was fabricated. The turn-on voltage was 8.7 V, and the maximum brightness, maximum current efficiency and luminescent efficiency were 142 cd/m^2 at 18.5 V, 0.06 cd/A and 0.019 lm/W at 10.2 V, respectively. When compared with the requirements in the progress of PLEDs, the

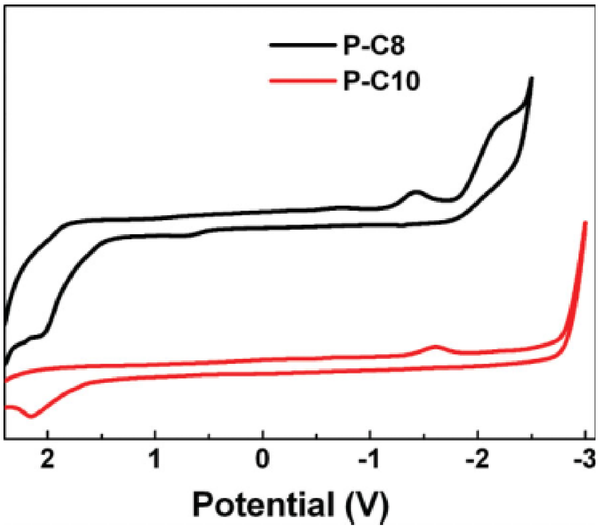

FIGURE 10 Cyclic voltammograms of films on a vitreous carbon electrode in 0.1 mol/L Bu_4NClO_4, acetonitrile solution. [Color figure can be viewed in the online issue, which is available at www.interscience.wiley.com.]

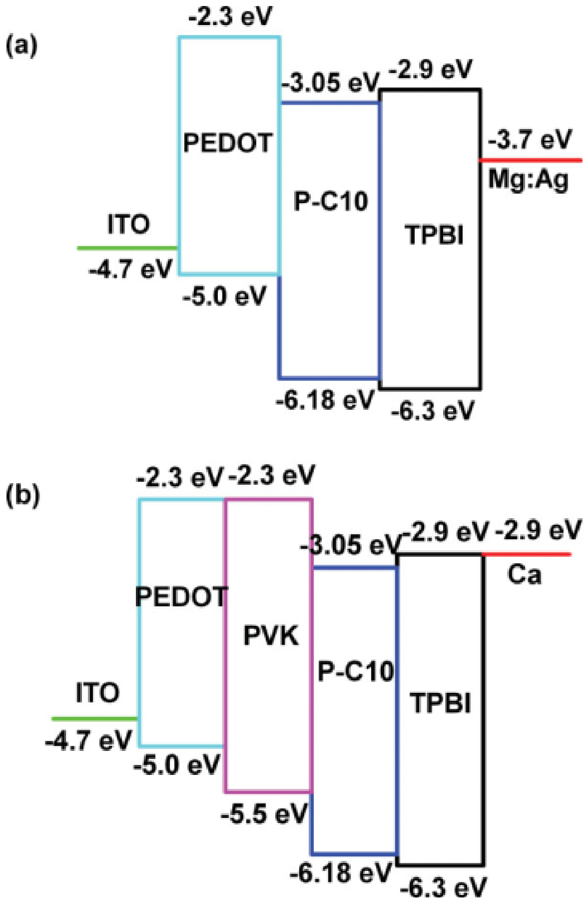

FIGURE 11 Energy level diagrams of device a (a) and device b (b). [Color figure can be viewed in the online issue, which is available at www.interscience.wiley.com.]

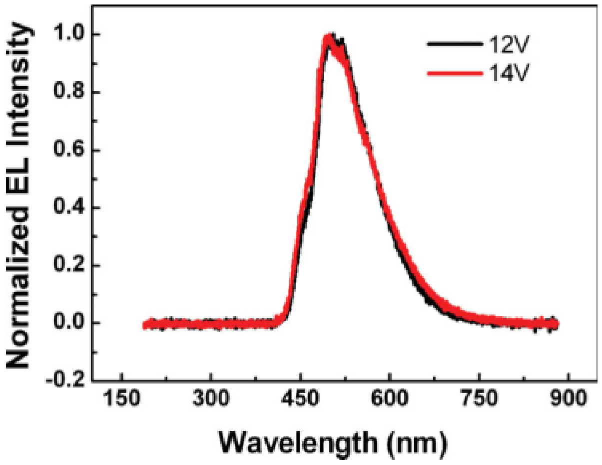

FIGURE 12 Normalized EL spectra of the device (ITO/PEDOT/PVK/polymer/TPBI/Ca/Ag) at different bias voltages. [Color figure can be viewed in the online issue, which is available at www.interscience.wiley.com.]

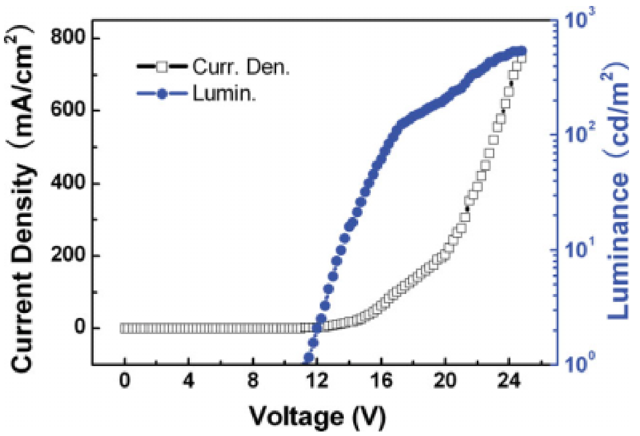

FIGURE 13 Current density-voltage and brightness-voltage characteristics of the EL device (ITO/PEDOT/PVK/polymer/TPBI/Ca/Ag) of P-C10. [Color figure can be viewed in the online issue, which is available at www.interscience.wiley.com.]

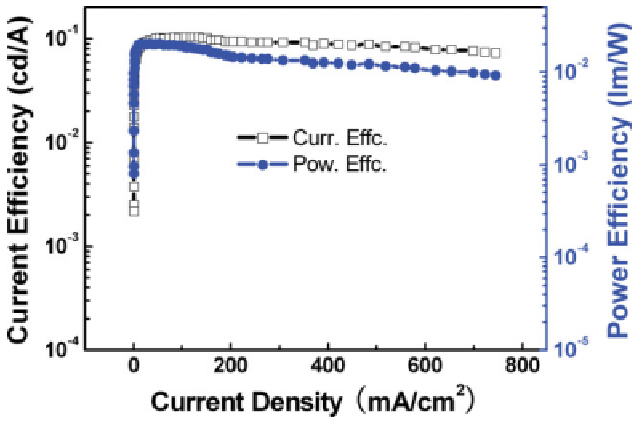

FIGURE 14 Current efficiency-current density and luminescent efficiency-current density characteristics of the EL device (ITO/PEDOT/PVK/polymer/TPBI/Ca/Ag) of P-C10. [Color figure can be viewed in the online issue, which is available at www.interscience.wiley.com.]

maximum brightness and efficiencies were too low to be used in actual application. According to electrochemical properties of P-C10, its HOMO energy level was −6.18 eV, which was much lower than that of PEDOT (−5.0 eV), so the energy barrier at the anode was about 1.18 eV, which might be difficult for the hole injection between the interface of PEDOT and polymer layers for device a. So poly(*N*-vinylcarbazole) (PVK), a well-known hole-transporting material in use for PLEDs, with HOMO and LUMO energy levels at −5.5 eV and −2.3 eV was introduced between PEDOT and P-C10 layers. Ca (work function = 2.9 eV) was better matched electrode than Mg (work function = 3.7 eV), and was used instead of Mg:Ag. So device b with the configuration of ITO/PEDOT/PVK/polymer/TPBI (15 nm)/Ca (25 nm)/Ag (80 nm) was fabricated to obtain better device performance. The energy level diagrams of the different layers of device a and device b were depicted in Figure 11. As shown in Figure 12, the EL spectra of device b had only one intense peak at 498 nm in the blue-green region, and there was almost no red shift with respect to the PL maximum emission in film state. The spectra exhibited good stability when the bias voltage was increased. The turn-on voltage was 11.4 V. Figures 13 and 14 showed the spectra of brightness and current density versus bias voltage and the spectra of current efficiency and luminescence efficiency versus current density of device b. The maximum brightness of device b was 541 cd/m^2. The maximum current efficiency and luminescent efficiency were 0.10 cd/A and 0.020 lm/W, respectively. It was concluded that the EL properties of device b was better than that of device a, as the brightness of device b was four times as that of device a, and the current efficiency as well as luminescent efficiency were both higher than those of device a, too. The addition of PVK layer facilitated the injection and transportation of holes from the anode, and the quantities of the electrons and holes increased largely, which caused the maximum brightness largely improved. The PVK layer may act the electron-blocking function, and then improve the balance of the electron and hole transporting, which enhanced the EL efficiencies of the device in a certain extent. The EL properties of device b were also much better than that of the MJLCPs containing electron-transport oxadiazole in side chains,[10] which indicated that the introduction of thiophene as hole-transport unit into the side chian of MJLCP and its directly connected way with the electron-transport oxadiazole was an efficient approach to impove the EL properties.

CONCLUSIONS

A series of electroluminescent MJLCPs with electron- and hole-transport units directly connected in the side chain were designed and synthesized for the first time, and their

TABLE 3 Electrochemical Properties of the Polymers

Polymer	λ_{edge} (nm)[a]	Optical E_g (eV)[b]	E_{ox}^{onset} vs. Ag/AgCl (V)	E_{red}^{onset} vs. Ag/AgCl (V)	E_{HOMO} (eV)	E_{LUMO} (eV)	Electrochemical E_g (eV)[c]
P-C8	446	2.78	1.66	−1.19	−6.07	−3.22	2.85
P-C10	427	2.90	1.77	−1.36	−6.18	−3.05	3.13

[a] λ_{edge} was the onset value of absorption spectrum in long wavelength range.

[b] Optical band gap was obtained from the empirical formula $E_g = 1240/\lambda_{edge}$ eV.

[c] Electrochemical $E_g = E_{ox}^{onset} - E_{red}^{onset}$ eV, $E_{HOMO} = -e\,(E_{ox}^{onset} - E_{1/2,\ FOC}) - 4.8$ eV, $E_{LUMO} = -e\,(E_{red}^{onset} - E_{1/2,\ FOC}) - 4.8$ eV

TABLE 4 Electroluminescent Properties of the Devices

Device	V_{on} (V)[a]	L_{max} (cd/m^2)[b]	Emission wavelength (λ_{em}, nm)[c]	Current efficiency (cd/A)[d]	Luminescent efficiency (lm/W)[e]	(*x*,*y*)[f]	EQE (%)
a	8.7	142	498	0.06	0.019	(0.270,0.445)	0.034
b	11.4	541	498	0.10	0.020	(0.270,0.445)	0.076

[a] Turn-on voltage at 1 cd/m^2.
[b] Maximum luminance.
[c] Emission wavelength at the bias voltage of 12 V.
[d] Maximum current efficiency.
[e] Maximum luminescent efficiency.
[f] 1931 CIE coordinate.

electroluminescent property and liquid crystalline property were discussed. The monomers were synthesized via seven steps and confirmed by various characterization techniques, and effective polymerization was realized. The polymers were characterized by thermal analysis, optical spectroscopy, cyclic voltammetry, electroluminescent analysis, PLM, 1D WAXD, 2D WAXD, and polarized photoluminescence. The resulting polymers possessed good thermal stability and high glass transition temperatures. The absorption spectra of both monomers and polymers had little red-shift in film than that in solution, indicating the aggregation was little. The photoluminescence spectra of the polymers and monomers in film had great red shift, suggesting the formation of excimer or exciplex. The polymers showed lower HOMO energy levels and LUMO energy levels than those of the MJLCPs containing oxadiazole unit reported before, which illuminated that the introduction of thiophene induced the electron transportation improved further and the HOMO energy level lower. Electroluminescence was studied with the optimized device configuration of ITO/PEDOT/PVK/polymer/TPBI/Ca/Ag. The maximum brightness and current efficiency reached 541 cd/m^2 and 0.10 cd/A, which proved that the introduction of thiophene and its directly connected way with electron-transport units could improve the EL property of side-chain conjugated polymers. The phase structures of the polymers were investigated with PLM, 1D WAXD, and 2D WAXD, and it was confirmed that the polymers formed smectic A phase after they entered liquid crystalline phase. Polarized photoluminescence measurements showed that the fluorescence intensity changed about 10 times when the polarized light entered in two perpendicular directions, which showed the potential utility for practical applications in display.

Financial supported by the National Science Foundation of China (Grant Nos.: 20634010, 20874002, 20874003, and 20974002).

REFERENCES AND NOTES

1 Grell, M.; Knoll, W.; Lupo, D.; Meisel, A.; Miteva, T.; Neher, D.; Nothofer, H. G.; Scherf, U.; Yasuda, A. Adv Mater 1999, 11, 671–675.

2 Yao, Y. H.; Yang, S. H.; Hsu, C. S. Polymer 2006, 47, 8297–8308.

3 O'Neill, M.; Kelly, S. M. Adv Mater 2003, 15, 1135–1146.

4 Zhao, N.; Botton, G. A.; Zhu, S.; Duft, A.; Ong, B. S.; Wu, Y. L.; Liu, P. Macromolecules 2004, 37, 8307–8312.

5 McCulloch, I.; Heeney, M.; Bailey, C.; Genevicius, K.; MacDonald, I.; Shkunov, M.; Sparrowe, D.; Tierney, S.; Wagner, R.; Zhang, W. M.; Chabinyc, M. L.; Kline, R. J.; McGehee, M. D.; Toney, M. F. Nat Mater 2006, 5, 328–333.

6 Rosen, B. M.; Wilson, C. J.; Wilson, D. A.; Peterca, M.; Imam, M. R.; Percec, V. Chem Rev 2009, 109, 6275–6540.

7 Zhou, Q. F.; Li, H. M.; Feng, X. D. Macromolecules 1987, 20, 233–234.

8 Zhou, Q. F.; Zhu, X. L.; Wen, Z. Q. Macromolecules 1989, 22, 491–493.

9 Zhu, X.; Yang, Q.; Zhou, Q. F. Chin J Polym Sci 1992, 10, 187–194.

10 Wang, P.; Chai, C. P.; Chuai, Y. T.; Wang, F. Z.; Chen, X. F.; Fan, X. H.; Xu, Y. D.; Zou, D. C.; Zhou, Q. F. Polymer 2007, 48, 5889–5895.

11 Yu, W. L.; Meng, H.; Pei, J.; Huang, W.; Li, Y. F.; Heeger, A. J. Macromolecules 1998, 31, 4838–4844.

12 Huang, W.; Meng, H.; Yu, W. L.; Gao, J.; Heeger, A. J. Adv Mater 1998, 10, 593–596.

13 Mochizuki, H.; Hasui, T.; Kawamoto, M.; Ikeda, T.; Adachi, C.; Taniguchi, Y.; Shirota, Y. Macromolecules 2003, 36, 3457–3464.

14 Chai, C. P.; Zhu, X. Q.; Wang, P.; Ren, M. Q.; Chen, X. F.; Xu, Y. D.; Fan, X. H.; Ye, C.; Chen, E. Q.; Zhou, Q. F. Macromolecules 2007, 40, 9361–9370.

15 Chen, S.; Gao, L. C.; Zhao, X. D.; Chen, X. F.; Fan, X. H.; Xie, P. Y.; Zhou, Q. F. Macromolecules 2007, 40, 5718–5725.

16 Stille, J. K. Angew Chem Int Ed Engl 1986, 25, 508–524.

17 Mentzel, U. V.; Tanner, D.; Tønder, J. E. J Org Chem 2006, 71, 5807–5810.

18 Boiteau, L.; Moroni, M.; Hilberer, A.; Werts, M.; Boer, B.; Hadziioannou, G. Macromolecules 2002, 35, 1543–1548.

19 (a) Willardson, R. K.; Weber, E.; Mueller, G.; Sato, Y. Electroluminescence I, Semiconductors and Semimetals Series; Academic Press: New York, 1999; (b) Bulovic, V.; Forrest, S. R.; Mueller-Mach, R.; Mueller, G. O.; Leslela, M.; Li, W.; Ritala, M.; Neyts, K. Electroluminescence II, Semiconductors and Semimetals Series; Academic Press: New York, 2000.

20 Zhang, D.; Liu, Y. X.; Wan, X. H.; Zhou, Q. F. Macromolecules 1999, 32, 5183–5185.

21 Xu, Y. D.; Yang, Q.; Shen, Z. H.; Chen, X. F.; Fan, X. H.; Zhou, Q. F. Macromolecules 2009, 42, 2542–2550.

22 Ye, C.; Zhang, H. L.; Huang, Y.; Chen, E. Q.; Lu, Y. L.; Shen, D. Y.; Wan, X. H.; Shen, Z. H.; Cheng, S. Z. D.; Zhou, Q. F. Macromolecules 2004, 37, 7188–7196.

23 Khanna, R. K.; Cui, H. Macromolecules 1993, 26, 7076–7078.

24 Yeh, K. M.; Chen, Y. J Polym Sci Part A: Polym Chem 2007, 45, 2259–2272.

25 Weder, C.; Wrighton, M. S.; Spreiter, R.; Bosshard, C.; Gunter, P. J Phys Chem 1996, 100, 18931–18936.

26 Weder, C.; Wrighton, M. S. Macromolecules 1996, 29, 5157–5165.

27 Jenekhe, S. A.; Osaheni, J. A. Science 1994, 265, 765–768.

28 Blatchford, J. W.; Jessen, S. W.; Lin, L. B.; Gustafson, T. L.; Epstein, A. J.; Fu, D. K.; Wang, H. L.; Swager, T. M.; MacDiarmid, A. G. Phys Rev B 1996, 54, 9180–9189.

29 Tekin, E.; Egbe, D. A. M.; Kranenburg, J. M.; Ulbricht, C.; Rathgeber, S.; Birckner, E.; Rehmann, N.; Meerholz, K.; Schubert, U. S. Chem Mater 2008, 20, 2727–2735.

30 Kawamoto, M.; Tsukamoto, T.; Kinoshita, M.; Ikeda, T. Appl Phys Lett 2006, 89, 121920–121920.

31 Kawamoto, M.; Mochizuki, H.; Ikeda, T.; Lee, B.; Shirota, Y. J Appl Phys 2003, 94, 6442–6446.

32 Kawamoto, M.; Mochizuki, H.; Ikeda, T.; Iino, H.; Hanna, J. J Phys Chem B 2005, 109, 9226–9230.

33 Hou, J. H.; Tan, Z. A.; Yan, Y.; He, Y. J.; Yang, C. H.; Li, Y. F. J Am Chem Soc 2006, 128, 4911–4916.

34 (a) Johansson, T.; Mammo, W.; Svensson, M.; Andersson, M. R.; Inganas, O. J.; Mater Chem 2003, 13, 1316–1323; (b) Chen, W. C.; Liu, C. L.; Yen, C. T.; Tsai, F. C.; Tonzola, C. J.; Olson, N.; Jenekhe, S. A. Macromolecules 2004, 37, 5959–5964; (c) Neher, D. Macromol Rapid Commun 2001, 22, 1365–1385; (d) Yang, Q.; Jin, H.; Xu, Y. D.; Wang, P.; Liang, X. C.; Shen, Z. H.; Chen, X. F.; Zou, D. C.; Fan, X. H.; Zhou, Q. F. Macromolecules 2009, 42, 1037–1046.